Observation of Jovian Decameter Waves at Mt. Zao Observatory using 40M Base Line Interferometer System

Sci. Rep. Tôhoku Univ., Ser. 5, Geophysics, Vol. 23, Nos. 3-4, pp. 133-148, 1976.

Observation of Jovian Decameter Waves at Mt. Zao Observatory Using 40M Base Line Interferometer System

HIROSHI OYA, AKIRA MORIOKA and MINORU KONDO

Upper Atmosphere and Space Research Laboratory
Tohoku University, Sendai 980, Japan

(Received March 27, 1976)

Abstract: Interferometric observation of Jovian decameter waves with two-elements Yagi antenna of 40 m span has been started at Mt. Zao Observatory of Upper Atmosphere and Space Research Laboratory, Tohoku University from Dec. 6, 1975. The source position of the arriving decameter waves is identified by sweeping the beam direction using a newly developed variable phase system where the phase difference between the two antennas is swept through the electronic circuits. The results give a confirmation that the decameter waves arrive at the antenna starting from Jupiter. The components of the emissions generated from the earth's surface such as the atmosphereics or interferences of broadcast waves are discriminated clearly from the Jovian decameter waves.

1. Introduction

Since the first identification of the Jovian decameter wave emissions (Burke and Franklin, 1955), the observations have been continued over a quarter of the century at several observation stations (Carr, 1961; Ellis, 1965; Warwick, 1967; Alexander, 1967). Though the age of the astronomical interests has been completed for the Jovian decameter waves during this quarter of the century, a new interests and objectives are raised in recent years, since the spacecrafts were sent into the Jovian magnetosphere (see the issues in Journal of Geophysical Research Vol. **79**, 1974). The new subjects are relating to the usage of the Jovian decameter waves as a messenger of the Jovian ionospheric events where the decameter waves are generated as a result of the Jovian magnetosphere disturbances (Oya, 1974; Scarf, 1974). For this purpose a new observation station has been started at Mt. Zao Observatory of Upper Atmosphere and Space Research Laboratory, Tohoku University (Oya, *et al.* 1975).

Observations of Jupiter decameter are required to discriminate from the interference of the emissions that are originated from the galaxy. One of the possible choice is to use multi-element Yagi antennas that has a narrow and sharp beam. The multi-element Yagi antenna should be drived tracking the sources mechanically. The mechanical driving system is subjected to heavy duties since the antenna elements have the length with the order of 10 m for the reception of the decameter waves. The interferometer system, however, has the possibility to scan the effective direction, for the reception of the decameter wave, by using electronric circuits without mechanical driving of the heavy antenna elements.

A new system for the interferometric observation has been developed for the

accurate detection of the Jovian decametric waves discriminating from the other noise sources using 40m-span interferometer system, that consists of two channels for the detection of the direction angle with respect to the local North-South direction, and for the detection of the direction angle with respect to the local East-West direction. The purpose of this paper is to give a technical report on the developed interferometric system and to give a preliminary report on the observation data that are selected from the series of the Jovian decameter wave emissions.

2. Principle and Instrumentation

Each channel of interferometer system consists of two antenna that are located with a span of 40 m; each antenna consists of two-elements Yagi antenna with vertically fixed axis (see Figure 1). Two channels are distributed in the local North-South direction and in the local East-West direction as has been given in Figure 2.

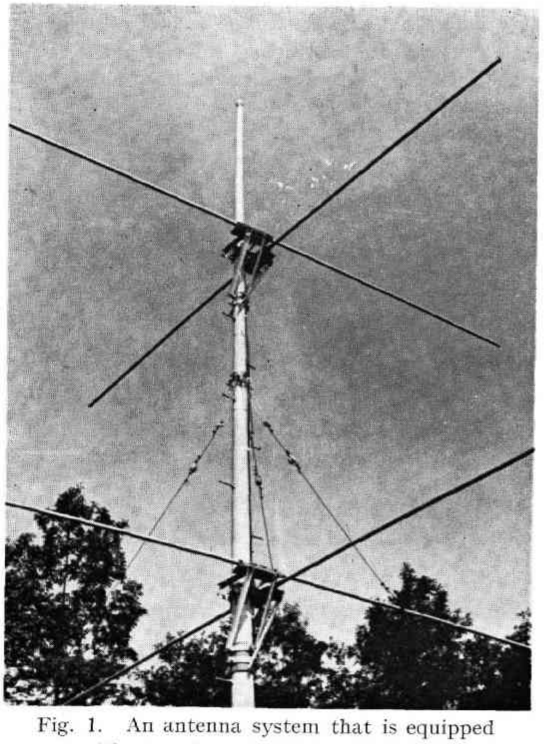

Fig. 1. An antenna system that is equipped with two-element Yagi antenna whose elements are crossed orthogonally.

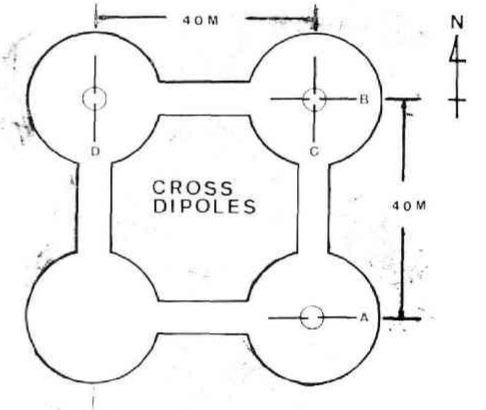

Fig. 2 Distribution of the antenna elements for the 40-m interferometer system. The antennas are used for two channels for the measurement of the directional angle with respect to the base line that is directed to the local North-South direction and for the measurement of the directional angle with respect to the base line that is directed to the local East-West direction.

A phase difference angle ϕ between the two antenna (between the element A and the element B, for an example), can be given by

$$\phi = \left(\frac{2\pi L}{\lambda}\right) \cos\theta \,, \tag{1}$$

where L, λ, and θ are the span length of the two antenna elements, the wavelength, and

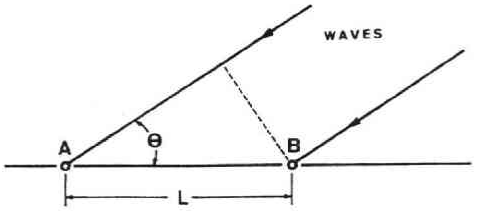

Fig. 3. Geometrical relation of the incident wave normal direction to the direction of the interferometer base line with a span, L.

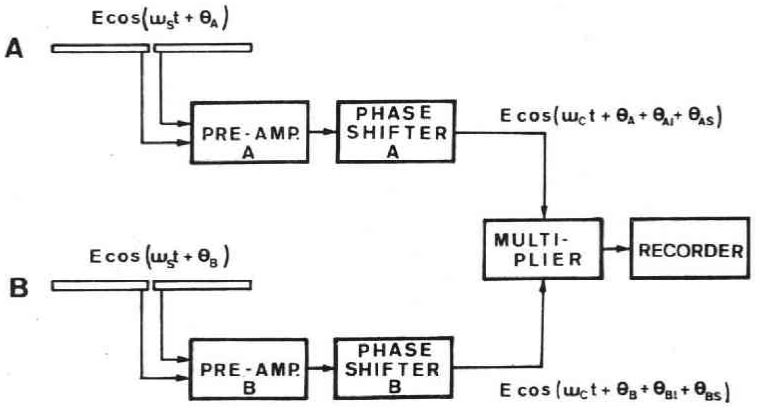

Fig. 4. A block diagram to illustrate the principle of the swept phase interferometric measurement system.

the direction angle of the arriving wave normal with respect to the vector of the base line direction (see Figure 3).

The Measurement of the ϕ value is made using a system as has been given in Figure 4. When the antenna A and B are excited by signals Ecos $(\omega_S t+\theta_A)$ and Ecos $(\omega_S t+\theta_B)$ (see Figure 4), the input signals to the multiplier are given by Ecos $(\omega_C t+\theta_A+\theta_{AI}+\theta_{AS})$ for the A-channel and by Ecos $(\omega_C t+\theta_B+\theta_{BI}+\theta_{BS})$ for the B-channel, where θ_{AI} and θ_{AS} are phase shifts in the electric circuits and the phase shift produced in the phase shifter, in the A-channel respectively; and θ_{BI} and θ_{BS} are the phase shift in the electric circuits and the phase shfit in the phase shfiter, in the B-channel, respectively. In both channels, the signal frequency ω_S is converted to ω_C due to frequency conversion of the super heterodyne receiving system. By multiplier, the signal is changed to the output signal E_0 that is given by

$$E_0 = \frac{aE^2}{2}\left[\cos\left(2\omega_C t+\theta_A+\theta_B+\theta_{AI}+\theta_{BI}+\theta_{AS}+\theta_{BS}+\theta_{BS}\right)\right.$$
$$\left.+\cos\left\{(\theta-\theta_B)+(\theta_{AI}-\theta_{BI})+(\theta_{AS}-\theta_{BS})\right\}\right], \qquad (2)$$

where a is a multiplying factor characterized by the instrument.

The output signal E_0 is reshaped using a filter that can pick up only a quasi-DC signal; i.e., the signal E_0^* is given by

$$E_0^* = \frac{aE^2}{2} \cos\{(\theta_A - \theta_B) + \Theta_I + \Theta_S\} \tag{3}$$

where $\Theta_I \equiv \theta_{AI} - \theta_{BI}$ and $\Theta_S = \theta_{SA} - \theta_{SB}$, respectively. By adjusting the phase shifter we can select to be that $\Theta_I = 0$. In this instrument, Θ_S is designed to vary with time, making a ramp function with respect to the time; i.e., using a constant Θ_0, it is given that

$$\Theta_S = \Theta_0(t - t_S), \text{ for } t_S < t < t_S + T, \tag{4}$$

where t_S and T are the arbitrary time and the repetition period, respectively. When Θ_S arrives at the condition

$$\Theta_S = \theta_B - \theta_A, \tag{5}$$

or

$$t = \frac{\theta_B - \theta_A}{\Theta_0} + t_S,$$

E_0^* takes a maximum value. The E_0^* value takes a negative maximum value at

$$\Theta_S = \theta_B - \theta_A + \pi, \tag{6}$$

or

$$t = \frac{\theta_B - \theta_A + \pi}{\Theta_0} + t_S.$$

When the E_0^* maximum value is observed at the time given by eq (5), therefore, the direction angle is given by

$$\theta = \cos^{-1}\left(\frac{\lambda}{2\pi L}\Theta_S\right); \tag{7}$$

the result is also given by

$$\theta = \cos^{-1}\left\{\frac{\lambda}{2\pi L}(\pi - \Theta_S)\right\}, \tag{8}$$

when we use the Θ_S value at the point where the E_0^* value takes the negative maximum. In the present instrumentation, the swept range of Θ_S is designed to cover from 0° to 180°. As has been depicted in Figure 5, we can measure the phase shift from 0° to 360° for θ_A–θ_B when we use both the positive maximum and the negative maximum of E_0^* values.

The overall system is shown in Figure 6. After the amplification through the pre-amplifiers, the signals are fed to the triple super heterodyne receiver in all the channels. The phase of the signal is swept at the second IF stage where the operating frequency is 3.010 MHz. The phase shifter is designed to be swept from 0° to 180° being controlled by the saw-tooth voltage that is fed to variable capacitor; the principal part of the phase control circuit is given in Figure 7. The control voltage to the phase shifter has two operation modes. One is a manual control signal that is designed to set a constant phase difference between A and B or C and D channels; the other is a sweep mode operation in which the control voltage is swept making a ramp function. The full sweep time of the control voltage is designed to be selective as 2, 4, 8 and 16 sec.

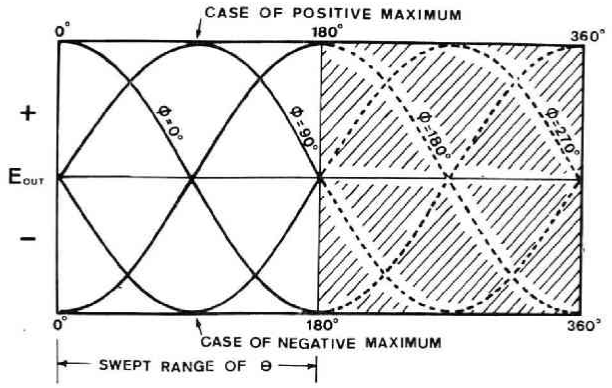

Fig. 5. The relation between the swept range of the phase angle and detected peak values of the interferometer output signal. The phase angle between 0° and 360° can be measured without phase sweep from 180° to 360° when the negative muximum point is used.

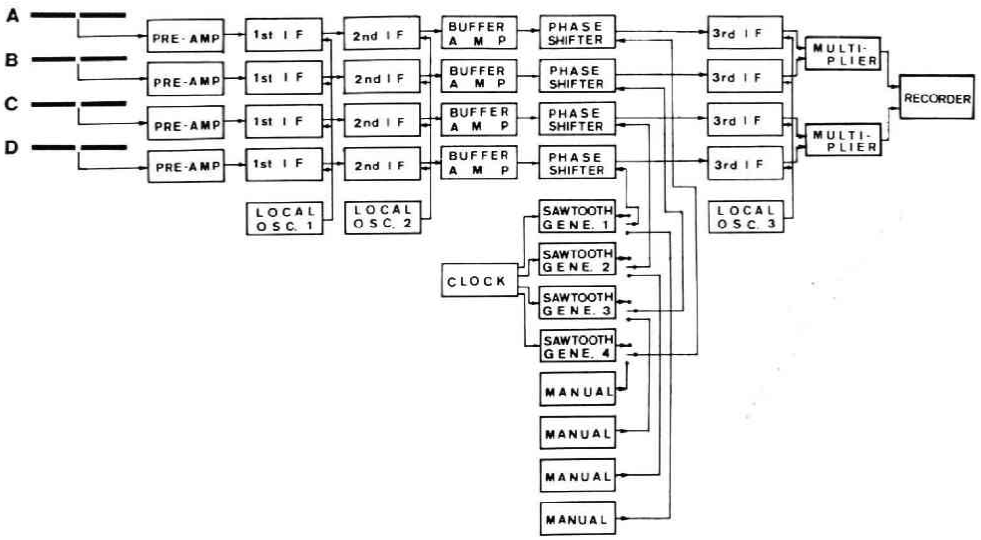

Fig. 6. Outline of the interferometer system that consists of the channel to find the directional angle with respect to the North-South base line (A-B channel) and of the channel to find the directional angle with respect to the East-West base line (C-D channel).

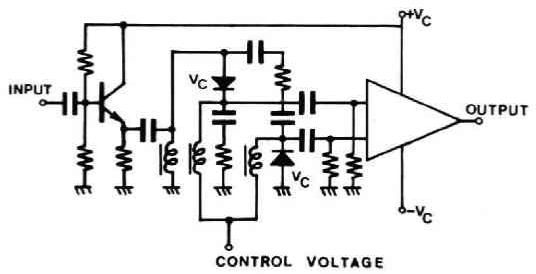

Fig. 7. Phase control circuit; the phase value is swept linearly by a saw tooth voltage that is applied to VC (variable capacitor).

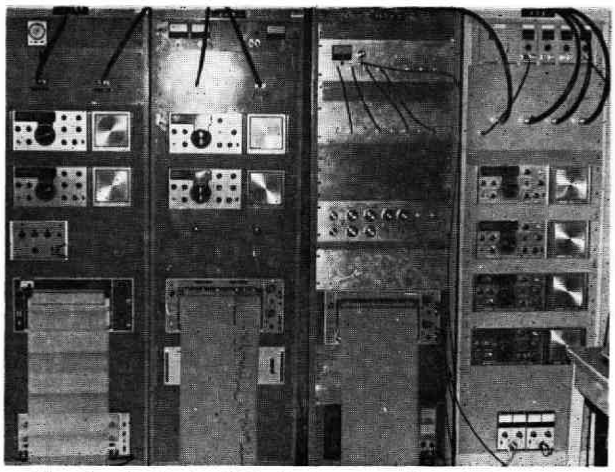

Fig. 8. Outlook of the instrumentation of the system.

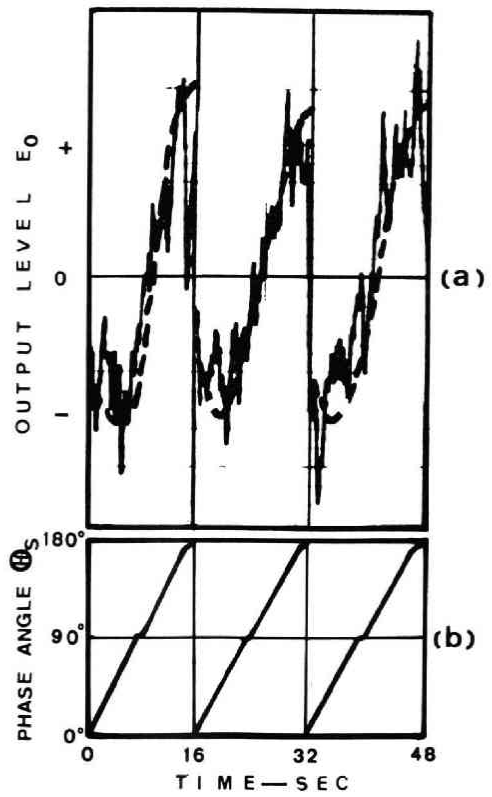

Fig. 9. Three examples of the swept phase interferometric observations (a) versus the swept phase angle (b).

The phaseshift angle Θ_S versus the voltage sweep time t is given in the bottom panel of Figure 9. In Figure 8, the overall view of the electric instruments of this phase swept interferometer system is given.

In figure 9, three samples of the swept interval for the interferometric observation of the Jovian decameter wave emissions are given; the signal is expressed using eq (3), as

$$E_0 = \frac{aE^2(t)}{2} \cos\{(\theta_A - \theta_B) + \Theta_S(t)\} . \tag{9}$$

As a reference, a curve that is given by

$$\bar{E}_0 = \frac{a\langle E^2\rangle}{2} \cos\{(\theta_A - \theta_B) + \Theta_S(t)\} , \tag{10}$$

where $\langle E^2\rangle$ is the average value of $E(t)$, is plotted in Figure 7 (see dashed lines). The result indicates that the average amplitude takes maximum value at $\theta_A - \theta_B + 180° = 0°$, i.e., $\theta_B - \theta_A = 180°$.

3. Examples of Observational Data Obtained on Dec. 6, 1975

The observation has started from Dec. 5, 2300 JST, in 1975. From Figures 10(a) to 10(g), a series of the observed data using the interferometer system is given from 0006 JST to 0046 JST on Dec. 6, 1975. The data are indicated being compared with the results obtained by the interferometric observation at 20.004 MHz (given by a notation "Phase" or "P" in Figures 10) with the results obtained by the single dipole antenna system at 19.980 MHz (given by a notation "Intensity" or "I" in Figures 10). The frequency difference between the two channels are 24 kHz that cannot be covered by the artificial communication system; i.e., the coincidence of the receptions between the two channels indicates that the decameter is emitted from the natural origin or the noise source other than broadcast waves. For the observation data of the Dec. 6, that are indicated from Figures 10(a) to 10(g), 90% of the coincidences between the 20.004 MHz channel and the 19.980 MHz channel are identified to be attributed to the Jovian decameter wave emissions as will be discussed in Sec. 4.

The vertical lines in the "Phase" or "P" channels indicate sections where the Θ_S is swept in a period of 16 sec. For the case of weak decameter wave emissions, the signal indicates a random noise-like variation as has been indicated in a period from 0008 JST to 0010 JST (see Figure 10(a)). The most possible source of this random shape decameter wave is thought to be in the galaxy. The most effective region for the decameter wave emissions of the galaxy is well known as the galactic center; in the period around 0000 JST on Dec. 6, however, we can observe only the rim region of the galaxy, where the weak decameter sources are distributed along the milky way. Therefore, no remarkable sinusoidal variation of the record is observed in this period.

i) From 0006 JST to 0010 JST (see Figure 10(a))

Among a galactic emissions several swept period with of remarkable emissions that

can be attributed to a defined source (i.e., Jupiter, for this case) are observed. One of the typical case of these emissions is given by a notation A (see Figure 10(a)).

ii) From 0011 JST to 0016 JST (see Figure 10(b))

Weak emissions from Jupiter are indicated around a period given by B (see Figure

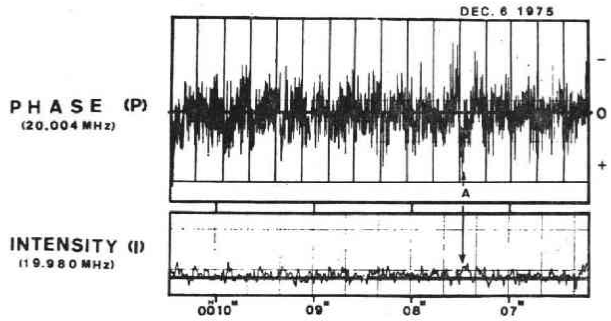

Fig. 10(a) The Jovian decameter waves observed by the interferometer (given in Phase or P channel) channel at 20.004 MHz and the intensity observed by the single dipole antenna at 19.980 MHz. The data are displayed for the interval from 0006 JST to 0010 JST on Dec. 6, 1975. A clear enhancement of the Jovian decameter waves are observed around a period given by A.

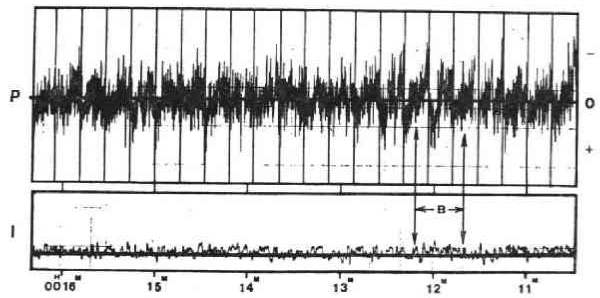

(b) Same as Figure 10(a). The data are displayed for the interval from 0011 JST to 0016 JST on Dec. 6, 1975. A remarkable enhancement of the Jovian decameter waves are observed around a period given by B.

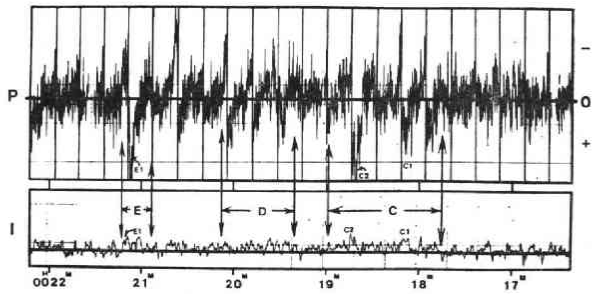

(c) Same as Figure 10(a). The data are displayed for the interval from 0017 JST to 0022 JST on Dec. 6, 1975. Strong emissions of Jovian decameter waves are observed in periods given by C,D, and E.

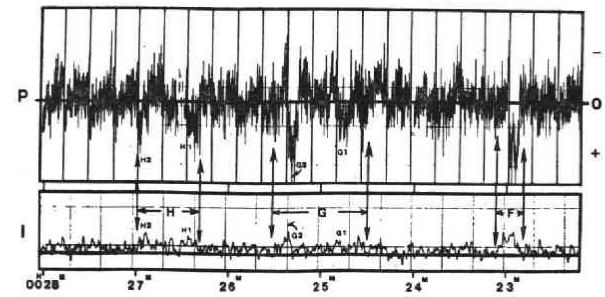

10(d) Same as Figure 10(a). The data are displayed for the interval from 0022 JST to 0028 JST on Dec. 6, 1975. Strong emissions of Jovian decameter waves are observed in periods given by F,G, and H.

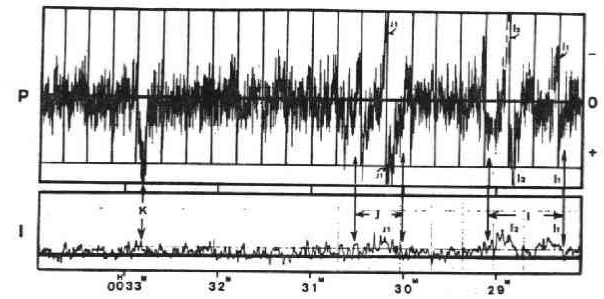

10(e) Same as Figure 10(a). The data in the period from 0028 JST to 0034 JST on Dec. 6, 1975 are displayed. One of the strongest part of this series of the event is given in the period I; the period J and the moment K give also very strong emissions.

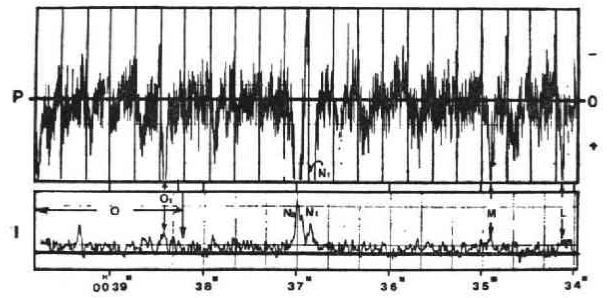

10(f) Same as Figure 10(a). The data in the period from 0034 JST to 0040 JST on Dec. 6, 1975 are displayed. Strong parts of the Jovian decameter waves are observed in the periods L,M,N and O; the emission at N_2 was identified as an atmospherics from the earth's surface.

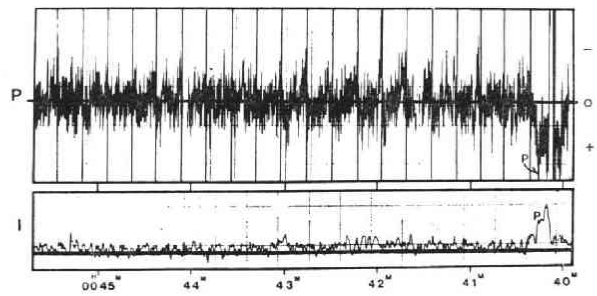

10(g) Same as Figure 10(a). The data in the last phase of the series of the Jovian decameter wave emissions are given here. The emission given by P was identified as an atmospherics from the earth's surface.

10(b)). A stochastic treatment may give the identification that the emission is coming from Jupiter in the period from 0014 JST to 0016 JST.

iii) From 0017 JST to 0022 JST (see Figure 10(c))

Strong emissions are obtained in this periods as indicated by intervals, C,D, and E. Corresponding to the peaks C1, C2, and E1 in 19.980 MHz channel, strong enhancements of the received signal are obtained in the interferometric measurement channel at 20. 0040 MHz, as have also been given by C1, C2, and E1.

iv) From 0022 JST to 0028 JST (see Figure 9(d))

The decametric emissions are increasing the power during this interval; we can see three periods F, G and H. The maximum emission of this time interval is given in the period F around 0023 JST, that is indicating that the source is located at the position corresponding to $\Theta_S=150°$. Four cases of strong emissions are obtained as given by G1, G2, H1 and H2.

v) From 0028 JST to 0034 JST (see Figure 10(e))

Largest emission of the series of Jovian decameter waves on Dec. 6 has been observed in this period. The case of maximum intensity is in an interval I corresponding to I_2; relatively large emissions are also observed as indicated by I_1, J_1 and K. The results in the periods I and J indicate that the decameter source can be identified corresponding to $\Theta(t)=180°$; since 180° is end point of the phase sweep, two peaks of the example jump from the positive maximum to the negative maximum values.

vi) From 0034 JST to 0040 JST (see Figure 10(f))

Four principal peaks in the 19.980 MHz channel make coincidence with the maximum intensities of interferometric observation as has been given by notations L, M, N_1 and O_1. Acase of interference due to atmospherics from the earth's atmosphere is observed at 0037 JST as given by N_2. This is decided as the source is located at the position other than the Jupiter since the position is largely off-set from the Jupiter as

will be discussed in Sec. 4.

vii) From 0040 JST to 0045 JST (see Figure 10(g))

Final phase on the series of the emissions are given in this interval. We can recognize that the signal terminates around 0043 JST, in the phase detection channel, when Jupiter is set over Mt. Zao. Near 0041 JST a strong interference due to atmospherics is recorded as has been given P, in Figure 10(g).

4. Identification of Jovian Decameter Emissions

The series of the observed data that has been described in Sec. 3 are plotted in terms of the direction angle θ_{EW} that is defined as the angle θ (see eq (1)) detected by the East-West component of the interferometer system. When the direction of Jupiter is given by an unit vector $\vec{d}$, θ_{EW} is given by

$$\theta_{EW} = \cos^{-1}(\vec{x} \cdot \vec{d}) \tag{11}$$

where $\vec{x}$ is an unit vector directed in the local East-West direction (directed to East from the observation point). Angle θ_{NS} is also defined as

$$\theta_{NS} = \cos^{-1}(\vec{y} \cdot \vec{d}) \tag{12}$$

where $\vec{y}$ is an unit vector directed in the local North-South direction (directed to North from the observation point). Using the azimuth ψ and the elevation angle ζ, therefore, the direction angle θ_{EW} and θ_{NS} are given as,

$$\begin{aligned} \theta_{EW} &= \cos^{-1}(\cos\psi \cdot \cos\zeta)\,, \\ \text{and} \quad \theta_{NS} &= \cos^{-1}(\cos\psi \cdot \sin\zeta)\,. \end{aligned} \tag{13}$$

On the series of data obtained on Dec. 6, 1975, observed θ_{EW} value are plotted versus the local time as given in Figure 11. In Figure 11, the strong emissions, that are labelled in Figures 10(a) ~ 10(g), are also plotted with the same labels corresponding to the records given in Sec. 3. The calculated θ_{EW} for the optical observation of Jupiter is also plotted as a trajectory in local time – direction angle (θ_{EW}) plane. Almost all the strong emissions detected by the interferometric observations are located close to the position of Jupiter, except for two cases (N_2 and P) that can be attributed to the atmospherics. In Figure 11, weak emissions of the wave phenomena given in Sec. 3 are also plotted using thin lines; these are indicating fluctuation from the center that is located at Jupiter. Thus, the results give a confirmation that the series of emissions described in Sec. 3 was transmitted from Jupiter, i.e., the waves are identified to be emitted from Jupiter.

From Figures 12(a) to 12(e), a series of Jovian decameter events in a observation interval from Jan. 23, 1976 to Feb. 21, 1976 is given. In all the cases observed on Jan. 23, (1976) Feb. 2, Feb. 9, Feb. 16 and Feb. 21, strong emissions (given by thick lines) are well indicating the coincidence with the trajectory of Jupiter that is plotted on planes that consists of local time (as ordinate) and the direction angle θ_{EW} (as abscissa).

Interference of signals originated at the earth's surface are also detected, these

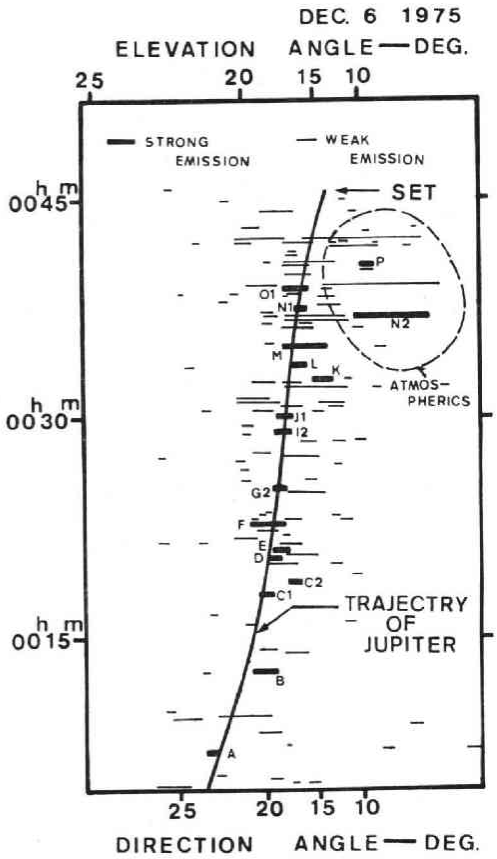

Fig. 11. Result of the interferometer observation carried out on Dec. 6, 1975; the format is given as the directional angle (θ_{EW}, for this case) versus the local time that is given in the ordinate. The observed peak values of the signal (including negative peaks) are plotted by piece of lines for the parts that are above (or below, for the case of the negative peak) a threshold value. The thick lines are used for the strong emissions and the thin lines are used to indicate the week emissions. The labels in the diagram are used corresponding to the labels used for the raw data given in Figures 10 to make dientification between the raw data and the plotted data. The results of the plotted data indicate that the directional angle of the emissions coincides with the direction angle of Jupiter.

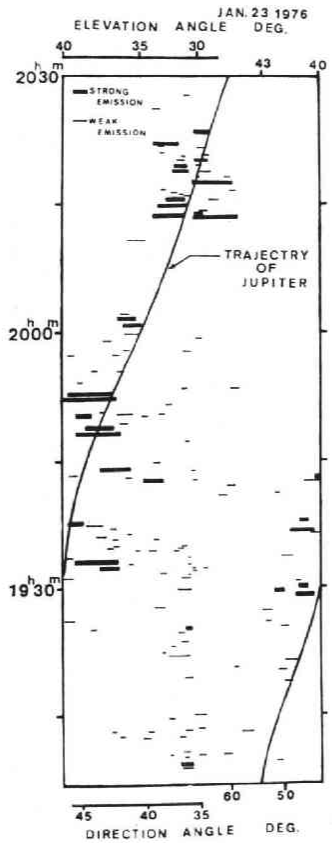

Fig. 12(a) Same as Figure 11 for the case observed on Jan. 23, 1976.

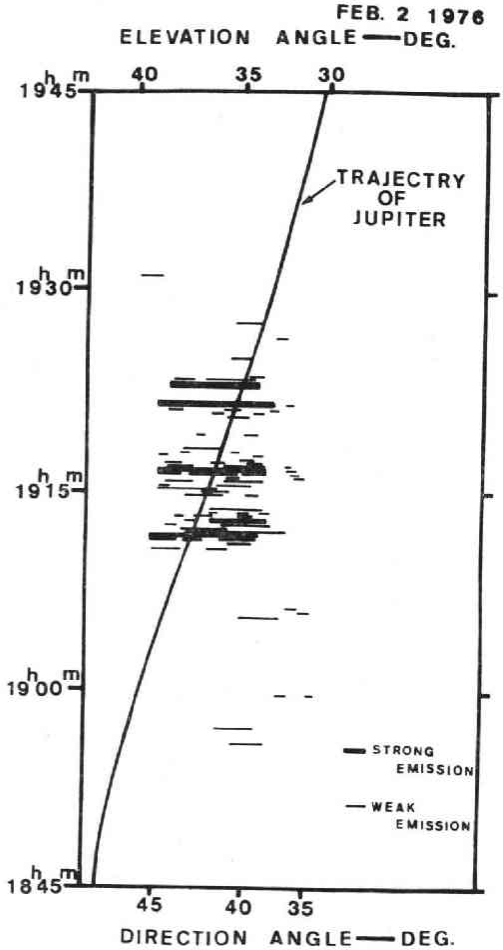

Fig. 12(b) Same as Figure 11, for the case observed on Feb. 2, 1976

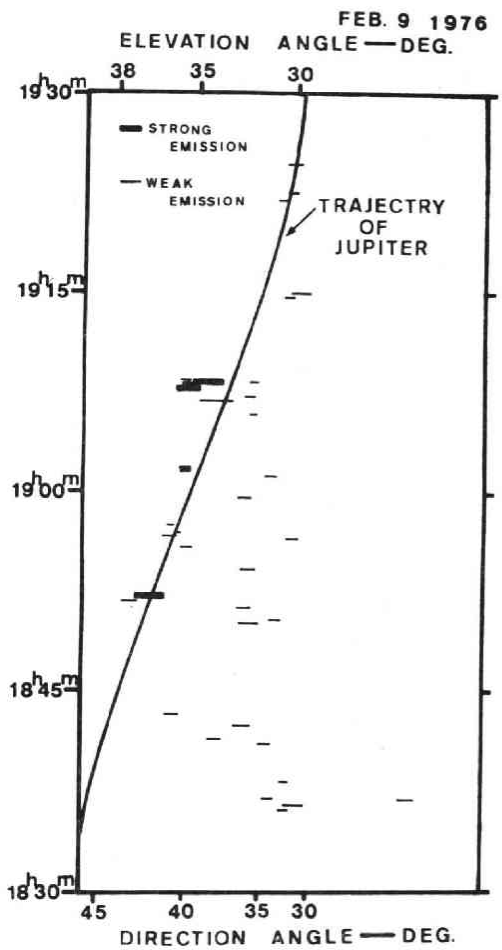

Fig. 12(c) Same as Figure 11, for the case observed on Feb 9, 1976.

are characterized by weak noises as indicated in the cases observed on Jan. 23 and Feb. 9 (see Figures 12(a) and 12(c)). The cross check with θ_{EW} and θ_{NS} data gives a complete confirmation on the identification of the Jovian decameter wave, and this check process discriminates the interference of the man-made signal. The interference of the man-made signal is identified on the data observed in an interval from 1850 JST to 1915 JST on Jan. 9, 1976. As have been indicated in Figures 13(a) and 13(b), the shift of the identified position for the observed wave data from the directional angle of the Jupiter, that is identified in Figure 13(a) in the interval from 1850 JST to 1915 JST, is clarified when we use the θ_{NS} data. That is, θ_{NS} data is indicating that the emissions around 1900 JST are observed only as an occasional coincidence with the direction of Jupiter for θ_{EW} data. Thus the interferometric observation system that consists of EW and NS channels is powerful tool to discriminate the interferences originated at the earth's surface from the Jovian decameter waves.

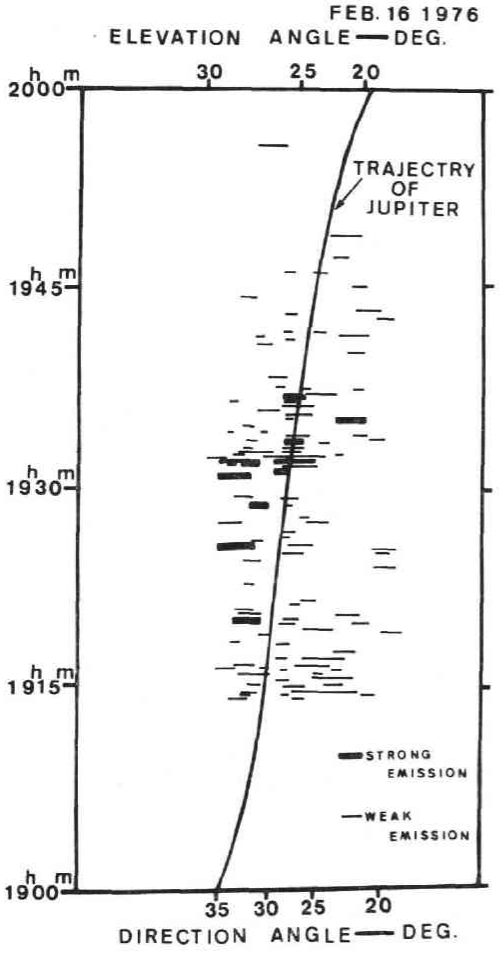

Fig. 12(d) Same as Figure 11, for the case observed on Feb. 16, 1976.

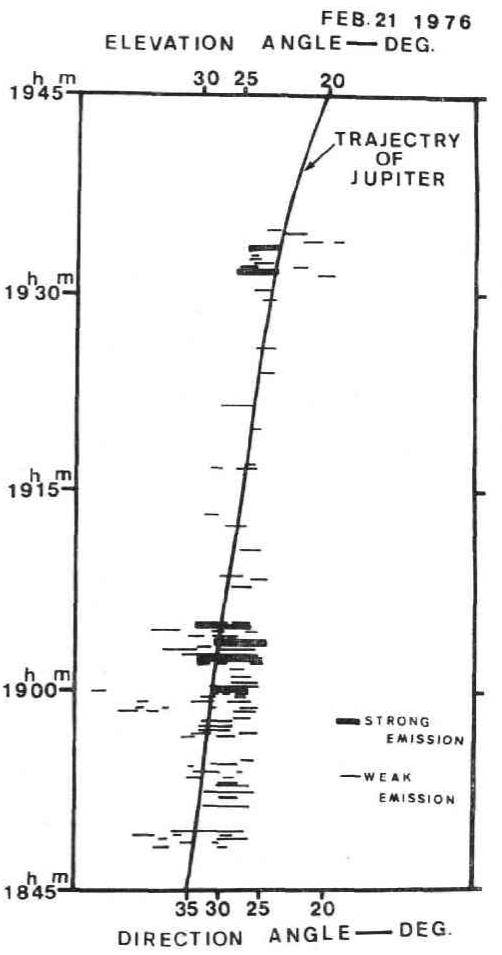

Fig. 12(e) Same as Figure 11, for the case observed on Feb. 21, 1976.

6. Conclusion

The interferometric observation of the Jupiter decameter wave observation has been started at Mt. Zao Observatory of Upper Atmosphere and Space Research Laboratory, Tohoku University. The interferometric observation system consists of two channels; one is for the observation of the direction-cosine with respect to the local East-West component, and the other is for the observation of the direction concerning with the local North-South component. Each channel consists of two Yagi antennas that are located with 40 m span. The phase differences of the signal received by elements of the interferometric observation channels are swept through the electric circuits where the phase shifters are controlled by the variable capaciters whose capacitance value is swept by saw-tooth voltage. By reading swept phase angle for the peak value of the detected signal the directional angles of the arriving Jovian

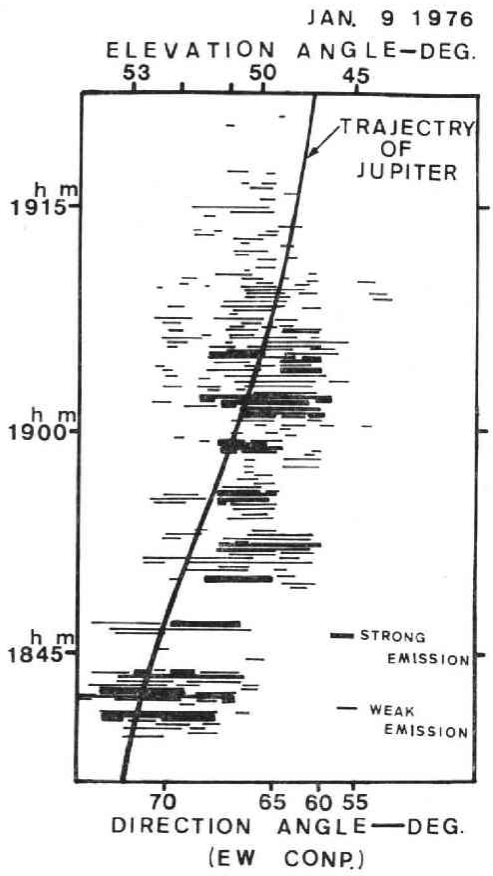

Fig. 13(a) Direction angle θ_{EW} given for the decameter wave emissions observed on Jan. 9, 1976 from 1835 JST to 1920 JST. The data format is same as given in Figure 12(a).

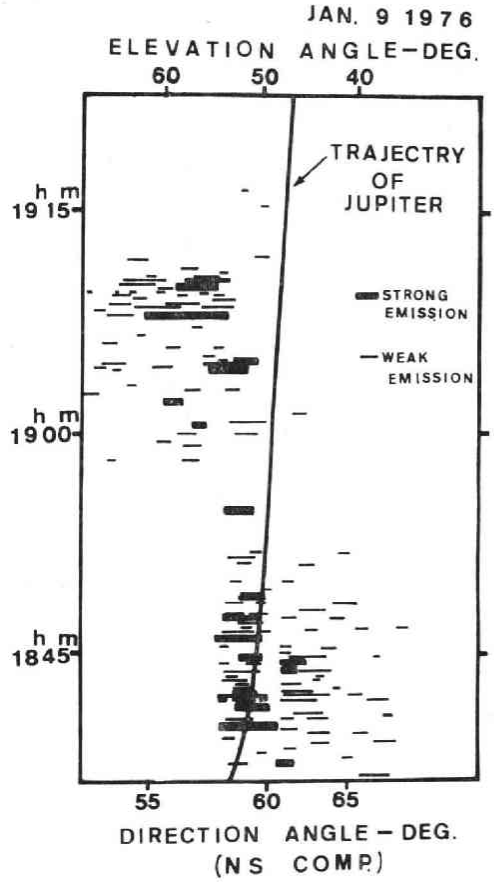

Fig. 13(b) θ_{NS} given in the same format as Figure 13(a). the comparison with the directional angle of Jupiter is concluded that the emission from 1850 JST to 1915 JST are emitted from a terrestrial origin.

decameter waves are identified.

The observation has been started on Dec. 6, 1975. Clear identifications have been made for the emissions at 20.0040 MHz indicating clear coincidence with the optical observation of the Jovian directional angle. The observation have also been made with comparison to the observation of the signal intensity at 19.980 MHz. All observation through the interferometric system reveals good coincidence with the intensity observation at 19.980 MHz. The interferometric observations give clear confirmation on the emission source and sharply improves the threshold for the detection of the Jovian decameter wave observation.

This system will give, hereafter, the data that give us the informations on the interactions of the solar wind with the Jovian magnetosphere; the interaction effects thought to be one of the origins of control factor of the Jovian decameter waves.

References

Alexander, J.K., 1967: NASA Rep. No-x-615-67-531

Bigg, E.K., 1964: Influence of the satellite Io on Jupiter's decametric emission, Nature **203**, 1008.

Burke, B.F., and K.L. Franklin, 1955: Radio emission from Jupiter, Nature **175**, 1074.

Carr, T.D., A.G. Smith, H. Bollhagen, N.F. Six, and N.E. Chatterton, 1961: Recent decameter wave-length observations of Jupiter, Saturn and Venus, Astrophys. J. **134**, 105.

Ellis, G.R.A., 1965: The decametric radio emissions of Jupiter, Radio Science **69D**, 1513.

Oya, H., 1974: Origin of Jovian decameter wave emissions-conversion from the electron cyclotron plasma wave to the ordinary mode electromagnetic wave, Planet Space Sci. **22**, 687.

Oya, H., A. Morioka, and M. Kondo, 1975: Reception of the Jupiter decameter waves at Mt. Zao observatory, Sci. Rep. Tohoku University Ser. **5**, Geophysics, **22**, 137.

Scarf, F.W., 1974: A new model for the high-frequency decametric radiation from Jupiter, J. Geophys. Res., **79**, 3835.

Warwick, J.W., 1967: Radiophysics of Jupiter, Sapce Science Review **6**, 841.